

NANO EXPRESS

Open Access



Morphological Effect of Non-targeted Biomolecule-Modified MNPs on Reticuloendothelial System

Xiao Li^{1,2}, Yan Hu^{1,2}, Jie Xiao^{1,2}, Dengfeng Cheng^{1,2}, Yan Xiu^{1,2*} and Hongcheng Shi^{1,2*}

Abstract

Magnetic nanoparticles (MNPs) with special morphology were commonly used as biomaterials, while morphological effects of non-targeted biomolecule-modified MNPs on biological behaviors were still unclear. In this research, spherical and rod-like Fe₃O₄ in a comparable size were synthesized and then surface-modified by bovine serum albumin (BSA) as a model of non-targeted biomolecule-modified MNPs. Morphological effects were featured by TEM and quantification of in vitro phagocytic uptake, as well as the in vivo quantification of particles in reticuloendothelial system (RES)-related organs of normal Kunming mice. For these non-targeted BSA-modified MNPs, intracellular distributions were the same, but the rod-like MNPs were more likely to be uptake by macrophages; furthermore, the BSA-modified MNPs gathered in RES-related organs soon after intravenous injection, but the rod-like ones were expelled from the lung more quickly and expelled from the spleen more slowly. These preliminary results may be referable if MNPs or other similar biomolecule-modified nanoparticles were used.

Keywords: Magnetic nanoparticles; Morphological effects; Reticuloendothelial system; Cellular uptake; Biodistribution

Background

Targeting delivery to diseased focus, as well as decreasing side effect to metabolic organs, is the main aim of nanoparticle-based drug delivery system. As an important item of biomedical materials, magnetic nanoparticles (MNPs) were often used as magnetic and biological targeting delivery system for theragnostic agents [1, 2]. For example, RGD-functionalized MNPs target for integrins of tumorous vascularization [3]; HIV-derived TAT-conjugated MNPs lead to efficient T cell labeling [4]. However, most nanoparticles concentrate in reticuloendothelial system for in vivo applications, decreasing targeting efficiency. On the other side, when being used in hyperthermia [5], accurate understanding of biodistribution is essential to avoid thermal injury to normal tissues.

Morphology heavily influences targeting efficiency, as well as pharmaceutical effects. Research on nanoparticle-based delivery systems with special morphology often

aims to extend cycling time, increase targeting efficiency, and decrease damage to normal tissues, so as to improve pharmaceutical effects. However, morphological effects on the uptake of reticuloendothelial system (RES)-related organs were often neglected. Hence, figuring out the morphological effect on biological behaviors is of pragmatic value for biomedical applications.

In this research, bovine serum albumin (BSA)-modified MNPs with similar size but different morphologies were synthesized to feature the corresponding morphological effect on reticuloendothelial system.

Methods

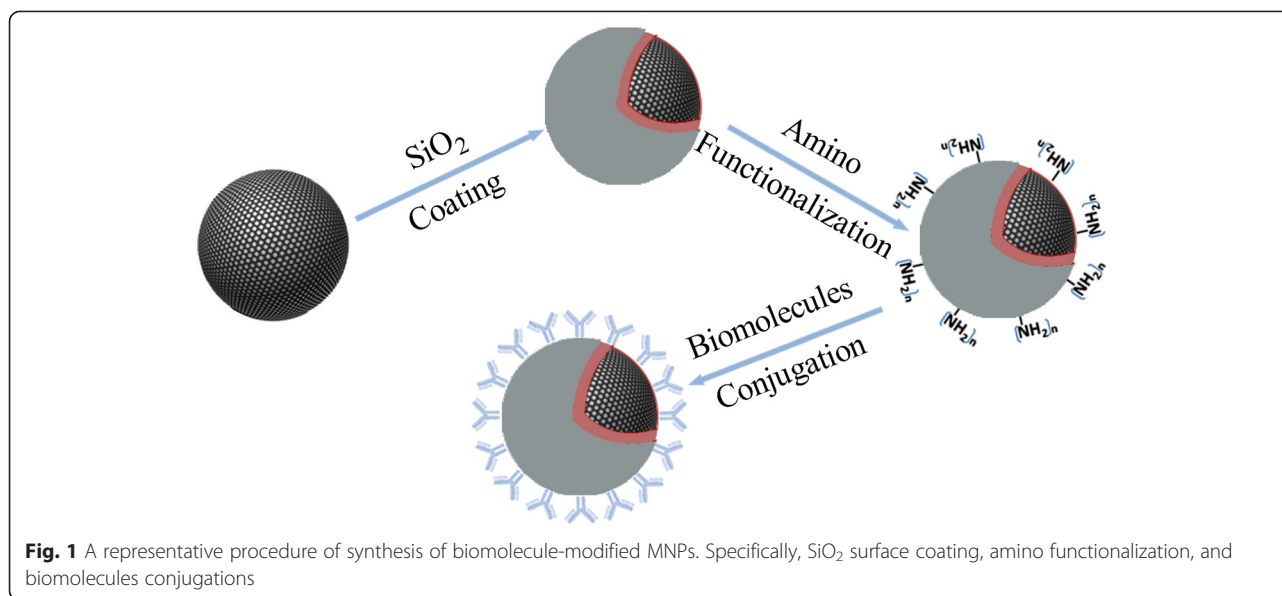
Synthesis of BSA-Conjugated MNPs

Spherical Fe₃O₄ was synthesized via hydrothermal method: 0.81 g FeCl₃·6H₂O and 1.47 g KAc were dissolved in 25 mL ethylene glycol and then treated by ultrasound for 1 min. The mixture was sealed in a 50-mL autoclave and maintained at 200 °C for 24 h. Product was washed by water and alcohol for three times and collected by a magnet. Rod-like Fe₃O₄ was synthesized following a reported hydrothermal method from Y. Liu [6]. According to G. Zhang's method (referred to Fig. 1), Fe₃O₄ was completely

* Correspondence: zsxuiyan@sina.com; shi.hongcheng@zs-hospital.sh.cn

¹Department of Nuclear Medicine, Zhongshan Hospital, Fudan University, Shanghai, China

²Shanghai Institute of Medical Imaging, Shanghai, China



covered by SiO₂ via alcoholysis of tetraethyl orthosilicate (TESO) in a mixed solution of methanol and methylbenzene (1:1, v/v) and then amino-functionalized via alcoholysis of N-(2-aminoethyl)-3-aminopropyltrimethoxysilane (AEAPS) [7]. Finally, BSA was conjugated to MNPs via reaction between amino groups and glutaric dialdehyde-activated amino-modified MNPs at 4 °C for 24 h. For in vivo tracking of MNPs' distribution, radiotracer-¹²⁵I was labeled to proteins: 3.7 MBq Na¹²⁵I and BSA-modified MNPs (1 mg MNPs contained) reacted for 5 min at 25 °C with the catalysis Iodogen.

X-ray diffraction (XRD) was performed at an operation voltage of 40 kV and a current of 40 mA with Cu K α radiation ($\lambda = 0.154056$ nm). TEM (operated at 200 kV) was used to picture the size and morphology of MNPs. FTIR was used to verify the existence of -NH₂; I-125 labeling rate was measured by radio-TLC with saline as the developing solvent. Stabilities in PBS and 10 % fetal bovine serum (FBS) were measured for 24 h at most.

Uptake Efficiency of BSA-Conjugated MNPs

Raw 264.7 macrophages were used for in vitro cellular uptake test. The macrophages were cultured in Dulbecco's Modified Eagle Medium (DMEM) with 10 % FBS at 37 °C in 5 % CO₂ atm. and seeded at 10⁵ cells/well in a 96-well plate. After 2 h incubation, the cells were exposed to a culture medium containing MNPs at 20 μ g/mL for 12 h at most. For cellular uptake test, unfixed nanoparticles were rinsed with 0.01 M PBS, and macrophages were then dissolved by HCl. Quantification of MNPs was determined via absorbance measurement of complex of ferrozine and ferrous ion at 562 nm and then corresponded to the standard curve. For TEM, the macrophages were fixed by 4 % paraformaldehyde, dehydrated by alcohol at gradient

concentration, embedded into epoxy resin, and then cut into slices of 75 nm.

In Vivo Biodistribution

Animal care and all experimental procedures were performed under the approval of the Animal Care Committee of Fudan University. Forty Kunming mice (male, 20 \pm 1 g) were selected for in vivo biodistribution research. The BSA-modified MNPs (0.74 MBq) were injected intravenously. The mice were sacrificed at 20 min, 1 h, 4 h, and 12 h (five mice for each group) after injection. RES-related organs were collected, weighted, and measured for radioactivity. Biodistribution was expressed as percentage of injected dose per gram (% ID/g), and differences between the spherical and rod-like particles were analyzed with paired *t* test.

Results and Discussion

Products from the two hydrothermal processes shared a same XRD spectrum of pure Fe₃O₄ (JCPDS No. 19-0629), meanwhile, the relevant stronger peak value of the rod-like Fe₃O₄ means an orientated growth along (311) crystal face. SiO₂ coating is amorphous, reflected by "bread"-shaped scattering peaks at around 25° (Fig. 2a, b). MNPs based on the different hydrothermal processes were totally different on morphology (Fig. 2c, d). The diameter of the spherical MNPs was 150–200 nm, while the length of the rod-like MNPs was 200–400 nm and has a diameter of 20–30 nm. SiO₂ coating covered the MNPs evenly with a thickness of <10 nm. The characteristic peak existed in 3380 and 3186 cm⁻¹ in FTIR spectrum proved the existence of -NH₂ after alcoholysis of AEAPS. I-125 was labeled to proteins stably with a radiochemical purity of >98 % and kept stable in PBS and 10 % FBS for

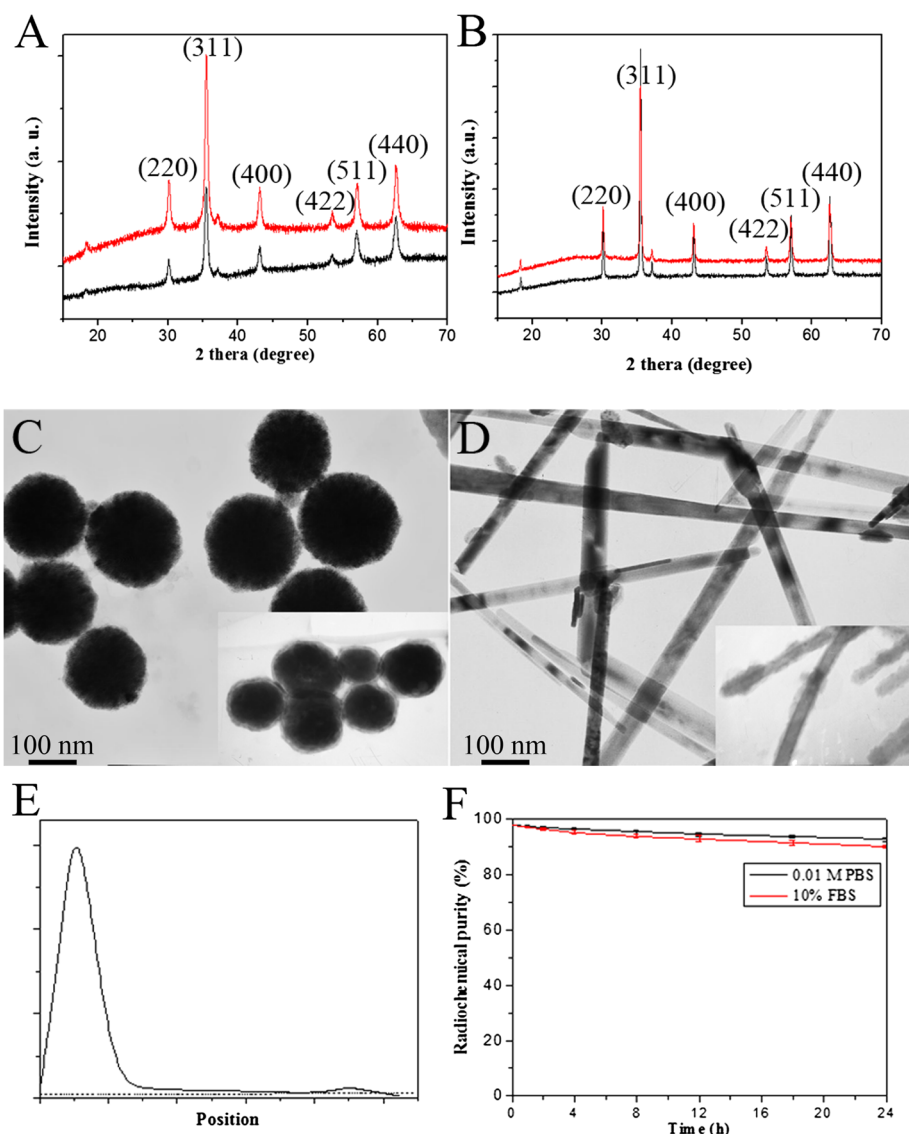


Fig. 2 Characteristics of BSA-modified MNPs. XRD spectrum of Fe_3O_4 and $\text{SiO}_2@\text{Fe}_3\text{O}_4$ (the red lines) for spherical MNPs (a) and rod-like MNPs (b). TEM of MNPs for spherical MNPs (c) and rod-like MNPs (d) with TEM of SiO_2 -coated MNPs on the lower right corner. Radio-TLC (e) and stability (f) of I-125-labeled BSA-modified MNPs

more than 24 h, guarantying truly reflection of in vivo biodistribution of BSA-conjugated MNPs (Fig. 2e, f).

Nanoparticle-based drug delivery systems are often spherical and with a diameter of 100–200 nm, such as the FDA-approved doxorubicin liposome (Doxil) and liposome-based Abraxane [8]. As a representative morphology, the rod-like MNPs were chosen to reflect the morphological effects on biological behaviors. The as-synthesized particles matched the optimal size for potential in vivo application. BSA was used as the non-targeted model of biomolecules, avoiding the confounding factor of targeting and emphasizing biodistribution resulted from morphological effects. I-125 was directly labeled to tyrosine of proteins; low-energy γ -ray can be easily

detected by a radio detector but does not lead to self-radiolysis [9].

In Vitro Cellular Uptake

These non-targeted particles were uptake via endocytosis mainly. The MNPs were observed in the cytoplasm in clusters, and nearly no MNPs entered the nucleus (Fig. 3a, b). There was a significant difference ($P < 0.05$) on uptake efficiency during the early period of uptake, but the difference tended to decline with time and changed to a non-significant difference ($P = 0.378$) after 12-h incubation (Fig. 3c).

Samir Mitragotri pointed out that morphology has a direct influence on endocytosis, promoting, inhibiting,

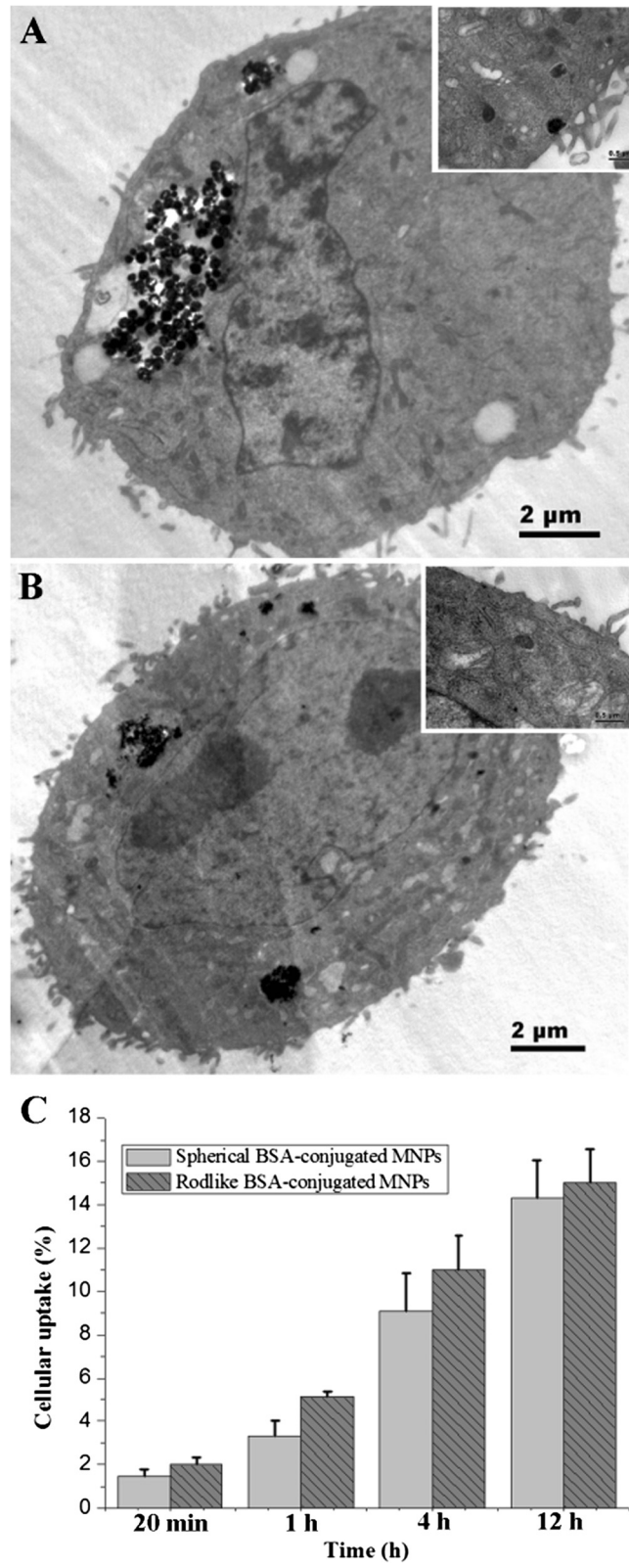
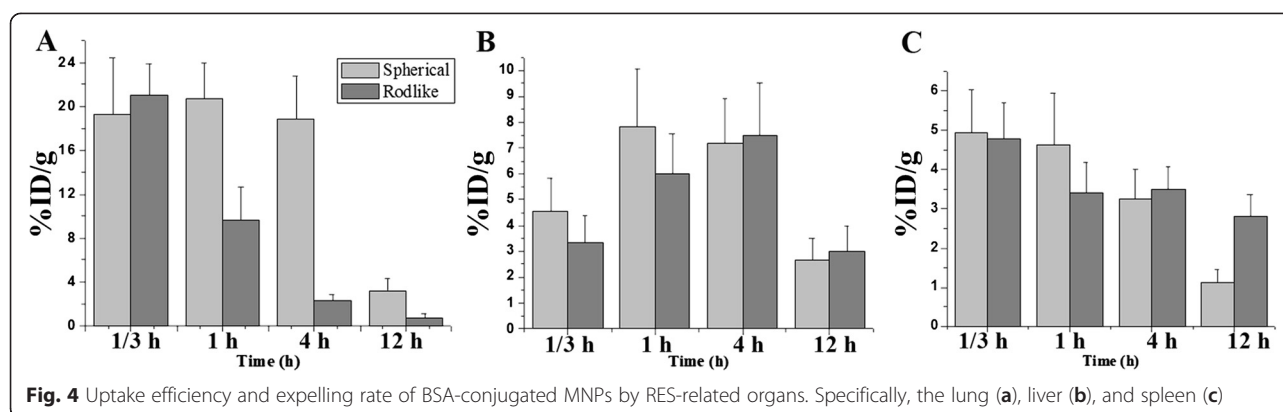


Fig. 3 TEM and quantification of cellular uptake. TEM of cellular uptake of spherical (a) and rod-like (b) BSA-modified MNPs. Quantification of cellular uptake (c)



and cellular uptake [10]. This minor in vitro difference observed above between the spherical and rod-like MNPs may be amplified for viviperception.

In Vivo Biodistribution

For in vivo biodistribution, MNPs gathered in RES-related organs soon after injection (19.2 % ID/g for the spherical ones, 20.9 % ID/g for the rod-like ones). Liver uptake got the peak value (7.8 % ID/g for the spherical ones and 7.6 % ID/g for the rod-like ones) at around 1–4 h after injection, and the particles were expelled at a similar rate. Due to the morphological effects, the rod-like BSA-modified MNPs were expelled from the lung more quickly, meanwhile, the rod-like particles were expelled from the spleen more slowly (Fig. 4).

Most non-targeted biomolecule-modified nanoparticles accumulated in the reticuloendothelial system because of endocytic effect of macrophages. Besides RES uptake, asialoglycoprotein receptor on hepatic cells which recognize galactose residues and acetyl galactosamine residues on biomolecules [11] partially contribute to uptake. Morphological effects were mainly reflected by metabolic differences on the expelling rate, which were resulted from the macrophages percentage composition and difference on microstructures of tissues. Taking the lung as an example, extraneous nanoparticles were easily held by pulmonary alveolus, but particles with special morphology tends to be released more quickly than the spherical ones. Hence, morphological effects, as well as targeting efficiency, should be overall considered when designing a biological targeting nanoparticle-based drug delivery system.

Conclusions

The BSA-modified MNPs with typical morphologies were synthesized. Both the spherical and rod-like biomolecule-conjugated MNPs gathered in RES-related organs soon, but the rod-like MNPs tend to be expelled from the lung more quickly but expelled from the spleen more slowly.

Competing Interests

The authors declare that they have no competing interests.

Authors' Contributions

XL, YX, and DC designed this research and drafted the manuscript. XL, YH, and JX did the in vivo and in vitro research. YX and HS did the data collections and statistics. All authors read and approved the final manuscript.

Acknowledgements

This work was financially supported by the National Science Foundation of China (81271608, 81201130), Shanghai Pujiang Program (13PJ1401400), Science Foundation of Shanghai (13ZR1439200), and Shanghai Municipal Commission of Health and Family Planning (XYQ2013106).

Received: 19 August 2015 Accepted: 8 September 2015

Published online: 17 September 2015

References

- Shubayev VI, Pisanic TR, Jin S. Magnetic nanoparticles for theragnostics. *Adv Drug Deliv Rev.* 2009;61:467–77.
- Panagiotopoulos N, Duschka RL, Ahlborg M, Bringout G, Debbeler C, Graeser M, et al. Magnetic particle imaging: current developments and future directions. *Int J Nanomedicine.* 2015;10:3097–114.
- Montet X, Montet-Abou K, Reynolds F, Weissleder R, Josephson L. Nanoparticle imaging of integrins on tumor cells. *Neoplasia.* 2006;8:214–22.
- Brooks H, Lebleu B, Vivès E. Tat peptide-mediated cellular delivery: back to basics. *Adv Drug Deliv Rev.* 2005;57:559–77.
- Hola K, Markova Z, Zoppellaro G, Tucek J, Zboril R. Tailored functionalization of iron oxide nanoparticles for MRI, drug delivery, magnetic separation and immobilization of biosubstances. *Biotechnol Adv.* 2015. doi:10.1016/j.biotechadv.2015.02.003.
- Liu Y, Gao Y, Guo F. Hydrothermal synthesis of magnetic Fe₃O₄ hexagonal and single crystal nanorods. *J Synth Cryst.* 2005;34:782–5.
- Zhang G, Liu Y, Zhang C, Hu W, Xu W, Li Z, et al. Aqueous immune magnetite nanoparticles for immunoassay. *J Nanoparticle Res.* 2009;11:441–8.
- Nishiyama N, Kataoka K. Current state, achievements, and future prospects of polymeric micelles as nanocarriers for drug and gene delivery. *Pharmacol Ther.* 2006;112:630–48.
- Su N, Dang Y, Liang G, Liu G. Iodine-125-labeled cRGD-gold nanoparticles as tumor-targeted radiosensitizer and imaging agent. *Nanoscale Res Lett.* 2015;10:160.
- Champion JA, Mitragotri S. Role of target geometry in phagocytosis. *PNAS.* 2006;103:4930–4.
- Zhang C, Qu X, Li J, Hong H, Li J, Ren J, et al. Biofabricated nanoparticle coating for liver-cell targeting. *Adv Healthc Mater.* 2015; doi:10.1002/adhm.201500202.